

## Green Synthesis and Characterization of Silver Nanoparticles from *Solanum tuberosum* Peel Waste: Efficacy Assessment through Antimicrobial and Antilarval Activities

Hamza Masood, Sania Riaz\*, Sherjeel Tariq, Syed Muhammad Hussain, Momina Shahid

Department of Bioinformatics and Biosciences, Capital university of Science and Technology, Islamabad, Pakistan.

Corresponding Author: Sania Riaz, E mail: [sania.riaz@cust.edu.pk](mailto:sania.riaz@cust.edu.pk)

### ABSTRACT

Silver nanoparticles serve as potent antimicrobial agents. In this study, we report the green synthesis of silver nanoparticles using *Solanum tuberosum* peel extract, followed by characterization via UV-Vis spectroscopy, SEM, and FTIR analysis. Antimicrobial efficacy against *Escherichia coli*, *Staphylococcus aureus*, and *Candida albicans* was evaluated using agar well diffusion, and activity of StAgNPs was compared with antibiotics like CAZ, TZP and NOR, with MIC and MBC values measured. Antilarval activity against *Aedes aegypti* larvae was also assessed. Results indicated successful nanoparticle formation (peak at 450 nm, 80–100 nm spherical particles) and notable antimicrobial and antilarval effects at higher concentrations. These findings highlight the non-toxic, eco-friendly potential of the green synthesized nanoparticles, with applications in antimicrobial therapies and vector control, although further validation is required.

**Keywords:** Silver nanoparticles; antimicrobial agents; *Solanum tuberosum* (potato peels); UV-Vis spectroscopy; SEM; FTIR; Gram-negative bacteria; *Pseudomonas aeruginosa*; *Staphylococcus aureus*; *Candida albicans*.

### INTRODUCTION

Nanobiotechnology is defined as the intersection of nanotechnology and biology, representing a rapidly emerging scientific discipline. It focuses on nanoparticles and nanoscale phenomena that have applications in biological systems. The prefix ‘nano’ derives from the Greek word *nanos*, meaning dwarf or extremely small, and denotes a billionth ( $10^{-9}$ ) of a unit. A nanometer is therefore one-billionth of a meter, making nanoparticles, the fundamental units of nanostructures, much smaller than objects encountered in daily life (Kale and Jagtap, 2018), (Kumar *et al.*, 2017).

Metallic nanoparticles have intrigued scientists for over a century and are now widely used in biomedical

sciences due to their diverse potential applications (Akhtar *et al.*, 2013). These particles can be synthesized and functionalized with chemical groups, enabling conjugation with antibodies, ligands, and drugs. Nanoparticles such as magnetic iron, gold, and silver are particularly prominent for their diagnostic, therapeutic, and antimicrobial capabilities (Ajitha *et al.*, 2018). Among these, silver nanoparticles (AgNPs) are of special interest because of their unique physical, chemical, and biological properties. While silver ions can be toxic, AgNPs can reduce toxicity while retaining antimicrobial activity. Nanoparticles typically range from 1 to 500 nm, and their high surface area maximizes antimicrobial activity and biological interactions (M. Grodzik *et al.*, 2017).

AgNPs exhibit notable physicochemical properties, including high electrical and thermal conductivity, chemical stability, and catalytic activity (Subbenaik, 2016). They demonstrate broad-spectrum bactericidal and fungicidal effects, making them valuable in consumer products such as plastics, soaps, pastes, food packaging, textiles, and water purification systems. In many applications, silver ions are released gradually through moisture-activated mechanisms, providing long-term antimicrobial protection (Quang Huy Tran *et al.*, 2013).

Silver nanoparticles can be synthesized using physical, chemical, or biological methods, broadly

### Article History

Received: [September 16, 2025](#), Revised: [November 25, 2025](#), Accepted: [December 10, 2025](#), First Online: [February 08, 2026](#).



Copyright: © 2026 by the authors. Licensee Roots Press, Islamabad Pakistan.

This article is an open access article distributed under the terms and conditions of the Creative Commons Attribution (CC BY) license.

<https://creativecommons.org/licenses/by/4.0/>

categorized into top-down and bottom-up approaches (as shown in **Figure 1**). Biological, or 'green,' synthesis utilizes plant extracts, bacteria, or fungi to

reduce silver ions, offering an eco-friendly and cost-effective alternative to conventional methods.

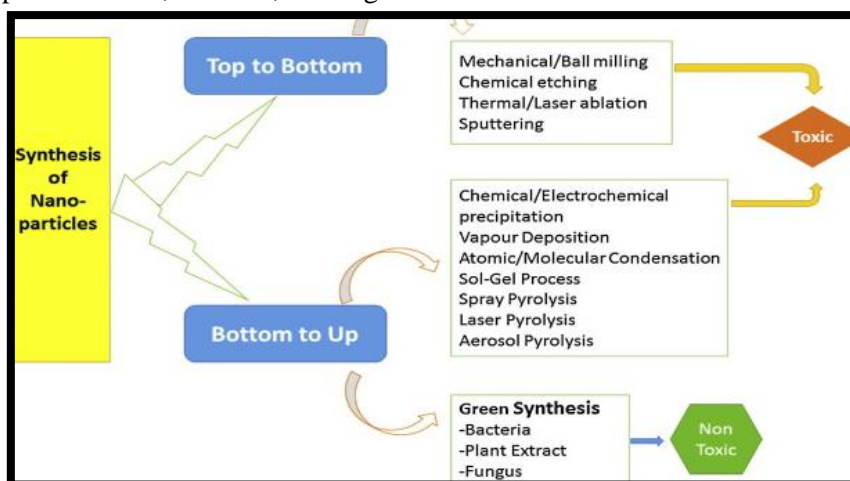


**Figure 1.** Bottom up and Top down approaches for the synthesis of nanoparticles (Ahmed *et al.*, 2016).

Green synthesis of nanoparticles is an emerging area of nanobiotechnology that employs environmentally benign materials for nanoparticle production. Plant-mediated synthesis offers advantages such as reduced toxicity, faster reaction times, and lower costs. Bioactive plant metabolites, including phenols, flavonoids, alkaloids, and terpenoids, not only contribute to human health but also act as reducing and stabilizing agents during nanoparticle synthesis. These bioactive compounds act chemically by donating electrons and stabilizing Ag ions by reduction. This study aims to synthesize AgNPs from *Solanum tuberosum* peel waste in a low-cost, energy-efficient manner, and to evaluate their antimicrobial and mosquitocidal activities. Also potato peel is a rich source of phenolic compounds (Gavarkar *et al.*, 2014), and also act as reducing and stabilizing agents for synthesis of silver nanoparticles from silver nitrate (Lakshmanan G *et al.*, 2017). The AgNPs will be characterized and tested for their antimicrobial and mosquitocidal activities.

## MATERIAL AND METHODS

### Nanoparticle Synthesis (StAgNPs)

Silver nanoparticles (StAgNPs) were synthesized via a green method using potato *Solanum tuberosum* peel waste. Fresh potatoes were purchased from a local market, and thoroughly washed with tap and distilled water to remove impurities before air-drying. A 10% extract was prepared by heating 10 g of potato peels in 100 mL of distilled water at 60 °C on hot plate for 30 minutes. The extract was filtered through Whatman filter paper and stored at 4 °C for later use (Tripathi & Sirohi).

A 10 mM silver nitrate (AgNO<sub>3</sub>) stock solution was prepared by dissolving 0.84 g of AgNO<sub>3</sub> in 500 mL of

distilled water and stored in a brown reagent bottle to avoid light exposure. The working solutions of 1, 5, and 10 mM were prepared by dilution of the stock. For synthesis, potato peel extract (Solution A) and 10 mM AgNO<sub>3</sub> solution (Solution B) were mixed in a 3:7 ratio and heated at 50 °C for 3 hours with continuous stirring. A visible color change from yellow to dark brown showing that StAgNPs may have formed as also reported by Gavarkar *et al.*, 2014. The mixture was centrifuged at 10,000 rpm for 10 minutes (as shown in Figure 2). Then pellet was washed three times with distilled water, and stored for characterization and bioassays.

### Methods for the Characterization of StAgNPs

#### Visual Observation

The formation of StAgNPs was initially monitored by visual color change. Reduction of Ag<sup>+</sup> ions was indicated by a shift from pale yellow to dark brown, attributed to surface plasmon resonance (Gavarkar *et al.*, 2014).

#### UV-Vis Analysis

Optical properties of StAgNPs were examined using a UV-Vis spectrophotometer at room temperature in diluted extract. (Specord 200 Plus, Germany). Absorbance was recorded in the 200–800 nm range, with distilled water as a blank reference (Ndikau *et al.*, 2017).

#### SEM Analysis

The morphology and size of StAgNPs were determined by scanning electron microscopy (SEM). A stock solution (1 mg/mL) was diluted 20-fold, and a drop was placed on a clean glass plate and air-dried and analyzed (Das *et al.*, 2017).

#### Fourier Transform Infra-Red Analysis

Fourier transform infrared (FTIR) spectroscopy was

performed to identify functional groups involved in nanoparticle stabilization. Absorption spectra were recorded to detect phytochemicals responsible for capping and stabilizing the StAgNPs (Ajitha *et al.*, 2018).

#### In Vitro Efficacy of Synthesized Silver Nanoparticle/ Antimicrobial Activity

The antimicrobial activity of StAgNPs was evaluated by the agar well diffusion method with well depth of 4.5mm. Muller Hinton Agar (MHA) was prepared, autoclaved, and poured into sterile Petri dishes. Wells (5 mm) were made, and bacterial and fungal test strains *E. coli*, *S. aureus*, *C. albicans* obtained from

CMH Rawalpindi were inoculated onto the media. Test samples were introduced into wells, and plates were incubated at 37 °C for 24 h. Antimicrobial activity was determined by measuring the inhibition zones in mm.

"MIC, MBC, and MFC were determined by broth dilution. Test tubes containing 5 mL nutrient broth were inoculated with 200 µL of microbial suspension and varying concentrations of StAgNPs (25–200 µg/mL). The lowest concentration inhibiting growth was considered the MIC, while bactericidal/fungicidal concentrations were recorded as MBC and MFC, respectively.

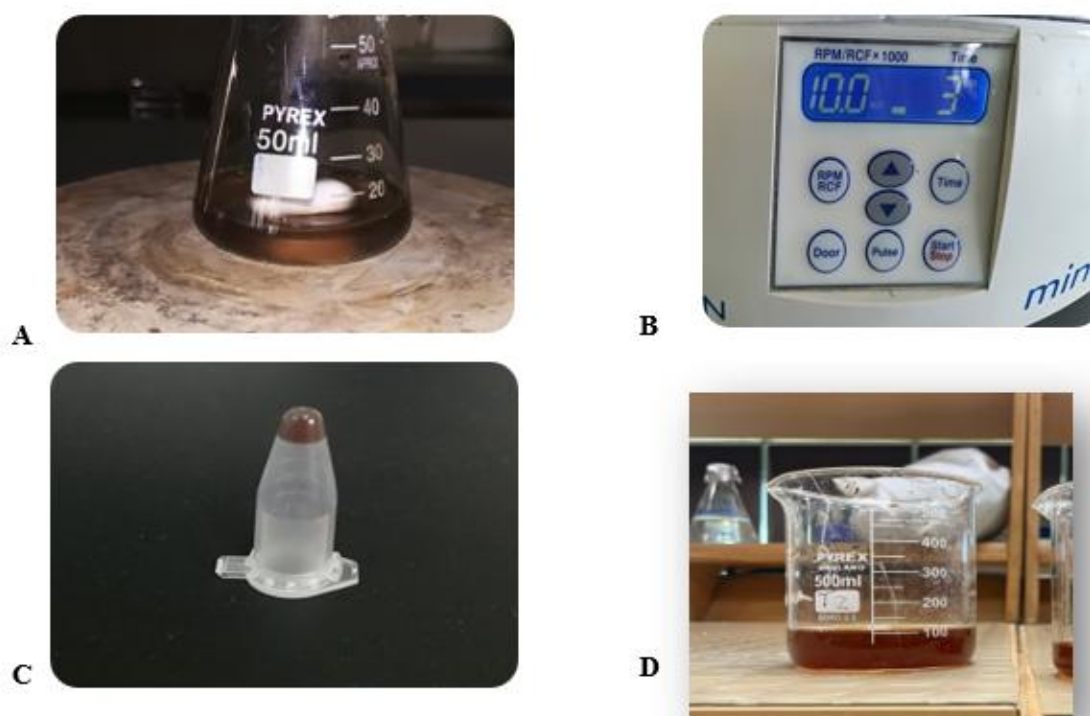


**Figure 2.** A. Formation of StAgNPs showing dark brown color, B. Centrifuge at 10000rpm for 3 min, C. Pellet after centrifugation, D; StAgNPs stored for further use.

#### Antilarval Activity

The Antilarval assay was performed using larvae of *Aedes aegypti*, collected from the Public Health Department, Islamabad. Test tubes (shown in Figure 3). Labeled as (control and 1-4) containing 5 mL distilled water were prepared and inoculated with

larvae. StAgNPs were added at increasing concentrations (100–1000 µg/mL). Larval survival was monitored at 12-hour intervals for up to 72 hours (Bhuvanewari *et al.*, 2016).

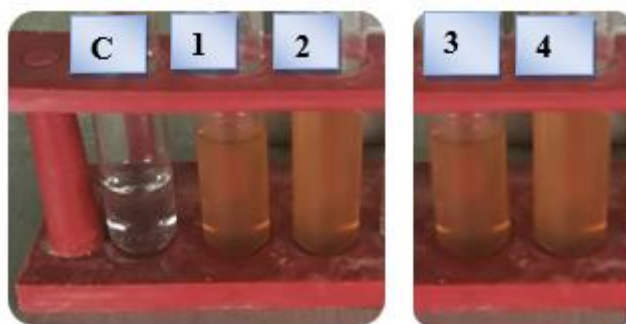


**Figure 3.** C-showing control without any StAgNPs and, 1-4 having StAgNPs in increasing order

**RESULTS**

**Synthesis of Silver Nanoparticles from *Solanum Tuberosum* Peel Extract**

StAgNPs were synthesized by mixing 10% potato peel extract (Solution A) with AgNO<sub>3</sub> solutions of varying concentrations (as given in Table 1), (1, 5, and 10 mM)

at different ratios and incubation conditions. No color change was observed in most combinations as being shown in Figure 4, except in the 3:7 ratio of extract to 10 mM AgNO<sub>3</sub> at 50 °C for 3 h, shown in Figure 6, where a distinct yellow-to-brown shift confirmed nanoparticle formation.

**Table 1.** Synthesis of StAgNPs by using different ratios of Solution A and B

| S. No | (A)ST Extract | (B) AgNO <sub>3</sub> | Time of Incubation | Temp of Incubation | Observation     |
|-------|---------------|-----------------------|--------------------|--------------------|-----------------|
| 1     | 3             | 7 (1mM)               | 3hrs               | 50                 | No color change |
| 2     | 3             | 7 (1mM)               | 24hrs              | Room               | No color change |
| 3     | 2             | 8 (1mM)               | 24hrs              | Room               | No color change |
| 4     | 2             | 8 (1mM)               | 3hrs               | 50                 | No color change |
| 5     | 3             | 7 (5mM)               | 3hrs               | 50                 | Light color     |
| 6     | 3             | 7 (5mM)               | 24hrs              | Room               | Light color     |
| 7     | 1             | 9 (5mM)               | 3hrs               | 50                 | No color change |
| 8     | 1             | 9 (5mM)               | 24hrs              | Room               | No color change |
| 9     | 3             | 7 (10mM)              | 24hrs              | Room               | Light color     |
| 10    | 3             | 7 (10mM)              | 3hrs               | 50                 | Dark brown      |
| 11    | 2             | 8 (10mM)              | 24hrs              | Room               | Light color     |
| 12    | 2             | 8 (10mM)              | 3hrs               | 50                 | Light color     |

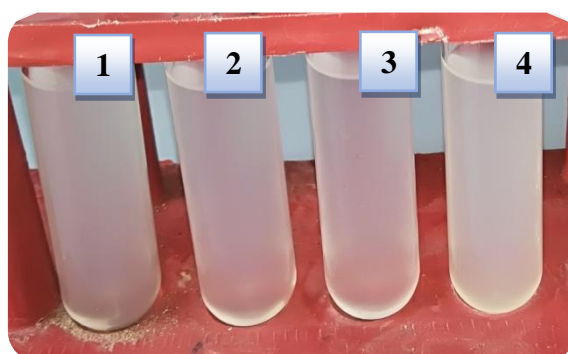


**Figure 4.** Mixing Soln A (1mM AgNO<sub>3</sub> ) and Soln B, showed no color change.

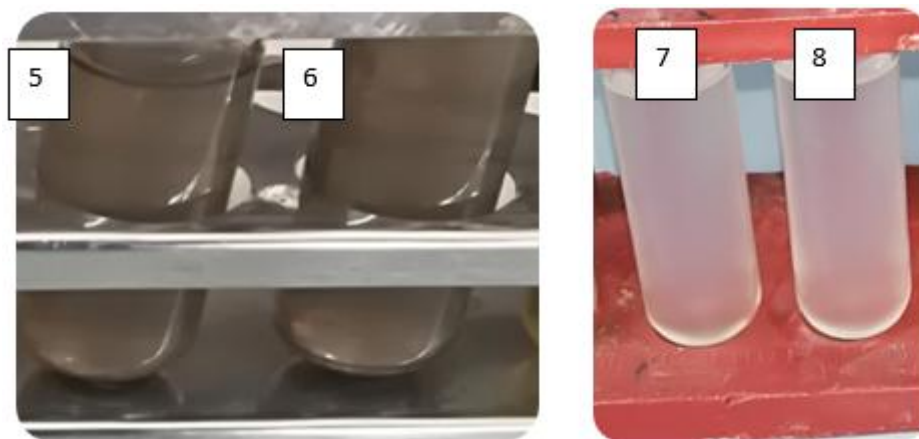


**Figure 5.** Showing Light color change in 5 and 6 while no color change in 7 and 8 after mixing Soln A (5mM AgNO<sub>3</sub>) and Soln B.



**Figure 6.** 10mM AgNO<sub>3</sub> was used and Dark brown color was appeared only in 10, while 9,11 and 12 are light in color.

**Characterization of AgNPs**  
**Visual Observation**

After mixing Soln A and Soln B, after heating the color of the solution changes from watery color to

yellow then to dark brown. As the ST extract extract was mixed in the aqueous solution of the silver ion then Ag<sup>+</sup> ions reduced into Ag<sup>0</sup>, which results in the color change into dark brown (as shown in **Figure 7**).

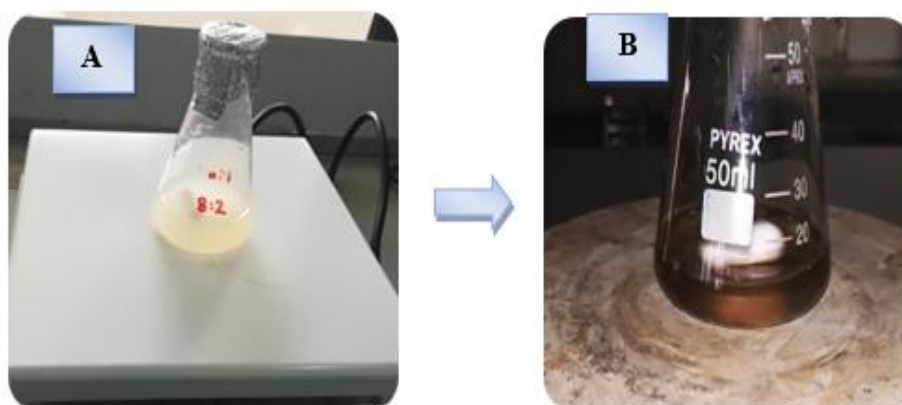


**Figure 7.** A showing light yellow color, B showing dark brown color indicating that StAgNPs are formed.

**UV-Vis Analysis**

UV–Vis analysis revealed a strong surface plasmon resonance peak at 450 nm (as shown in Figure 8),

consistent with the formation of AgNPs. Increased absorbance was observed over time, indicating progressive nanoparticle synthesis.

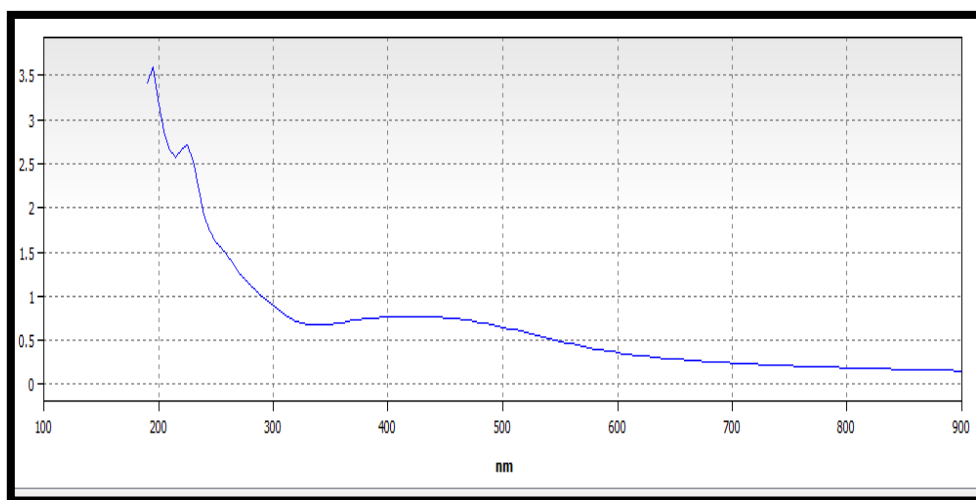


**Figure 8.** UV-Vis Spectra of AgNPs, showing strongest peak due to higher absorbance at 450nm.

### Scanning Electron Microscopy Analysis

The SEM imaging demonstrated that the synthesized nanoparticles were predominantly spherical (as

shown in Figure 9), with an average diameter of 80–100 nm (Pugazhendhi *et al.*, 2018).

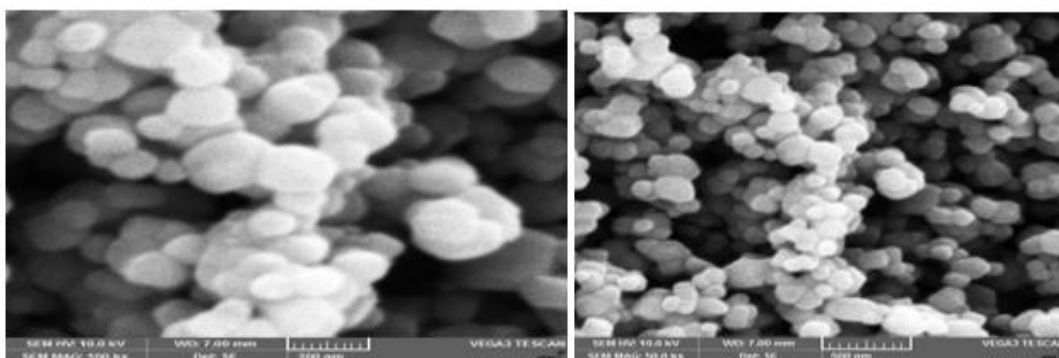


**Figure 9.** Image clearly shows the StAgNPs as Spherical in shape and approximately 80-100nm in size at 50kx and 100 kx resolution.

### Fourier Transform Infrared Spectroscopy

FTIR spectra showed prominent peaks at 3245.11  $\text{cm}^{-1}$  (phenolic OH stretch) and 1636.16  $\text{cm}^{-1}$  (aromatic alkenyl bending) as shown in Figure 10, confirming the involvement of phenolic compounds in the reduction and stabilization of AgNPs.

### Applications of Silver Nanoparticles

#### Antibacterial Activity

StAgNPs exhibited significant antibacterial activity against *E. coli* and *S. aureus*. At 100  $\mu\text{g}$  and 200  $\mu\text{g}$ , inhibition zones ranged from 16–20 mm and 19–21

mm, respectively (Table 2). StAgNPs produced larger inhibition zones compared to  $\text{AgNO}_3$  and crude peel extract, and their efficacy was comparable to standard antibiotics (TZP, NOR, CAZ) shown in Figure 11.

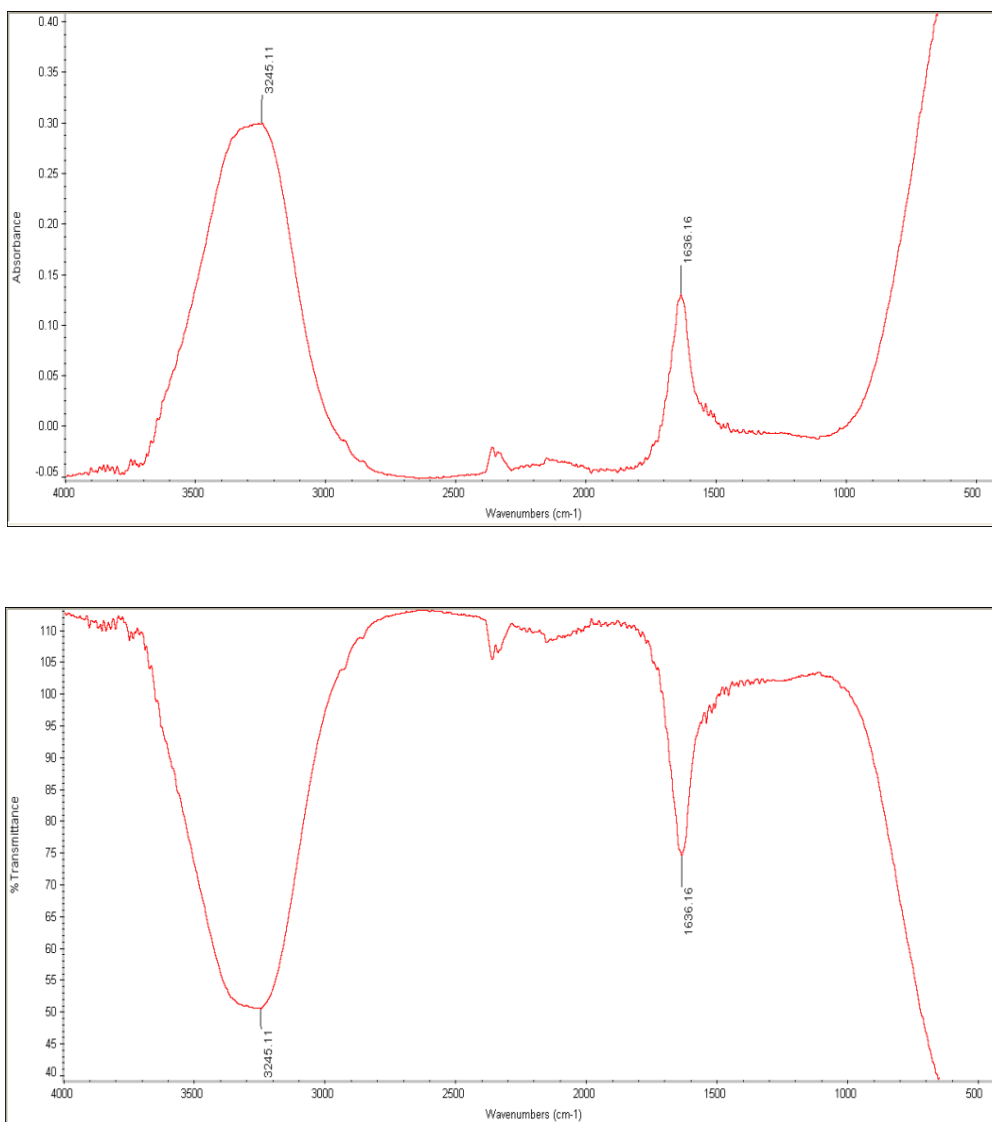


**Figure 10.** Showing FTIR results of StAgNPs, showing different peaks at 3245.11 phenolic OH stretch and 1636.16 Aromatic Alkenyl bending.

**Table 2.** The Zone of inhibitions of antibiotics, St-extract, AgNO3 and StAgNPs.

| S. No | Pathogen         | Zone of inhibition Antibiotics |           |      |                  | Zone of Inhibition |               |               |
|-------|------------------|--------------------------------|-----------|------|------------------|--------------------|---------------|---------------|
|       |                  | 1                              | 2         | 3    | 4                | 5                  | 6             | 7             |
|       |                  | TZP                            | CAZ       | NOR  | ST Extract 100µL | AgNO3 100µL        | StAgNPs 100µg | StAgNPs 200µg |
| 1     | <i>E. coli</i>   | 24mm                           | No effect | 19mm | No effect        | 22mm               | 16mm          | 20mm          |
| 2     | <i>S. aureus</i> | 25mm                           | No effect | 24mm | No effect        | 17mm               | 19mm          | 21mm          |

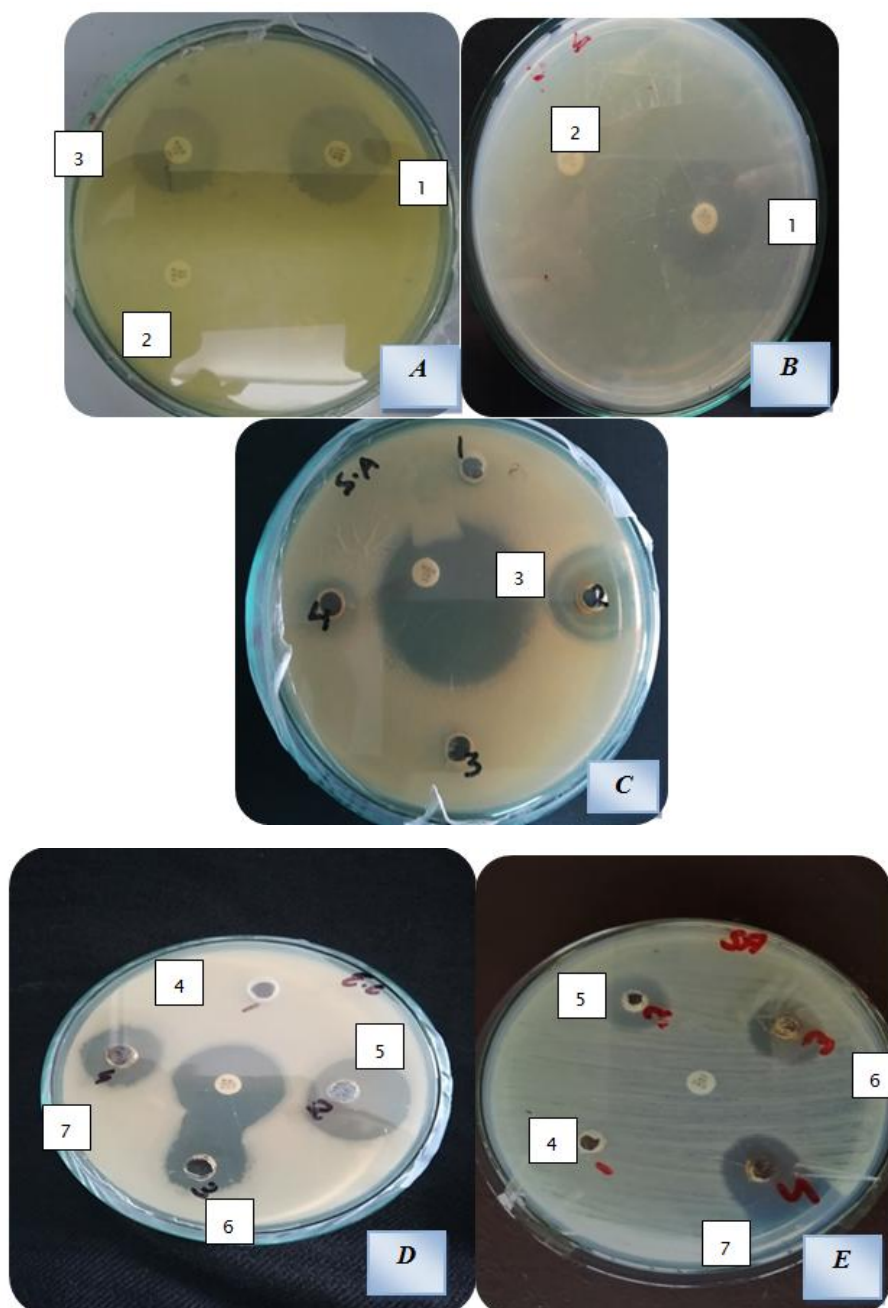


**Figure 11.** A, B and C; showing antibiotics zone of inhibition on *E. coli* and *S. aureus*, D and E; showing effects of ST extract, AgNO<sub>3</sub> and StAgNPs on *E. coli* and *S. aureus*.

**Antifungal Activity**

The green synthesized StAgNPs were also checked for antifungal activity using fungal strain *Candida albicans*. Their impact was assessed by comparing with the antifungal activity of antibiotics like piperacillin–tazobactam, ceftazidime, norfloxacin (TZP, CAZ, NOR) and also compared with St peel extract, AgNO<sub>3</sub> 10mM by measuring zone of inhibition (Table 3). StAgNPs were used at different concentrations like 25µg, 50µg, 100µg and 200µg but

100µg and 200µg show more activity and zone of inhibition shown in Figure 12.

**Table 3.** The Zone of inhibitions of antibiotics, St extract, AgNO3 and St AgNPs against *C. albicans*.

| S. No | Pathogen           | Zone of inhibition Antibiotics |           |      |                     | Zone of Inhibition |                  |                  |
|-------|--------------------|--------------------------------|-----------|------|---------------------|--------------------|------------------|------------------|
|       |                    | 1                              | 2         | 3    | 4                   | 5                  | 6                | 7                |
|       |                    | TZP                            | CAZ       | NOR  | ST Extract<br>100µL | AgNO3<br>100µL     | StAgNPs<br>100µg | StAgNPs<br>200µg |
| 1bv   | <i>C. albicans</i> | 24mm                           | No effect | 16mm | No effect           | 19mm               | 15mm             | 18mm             |

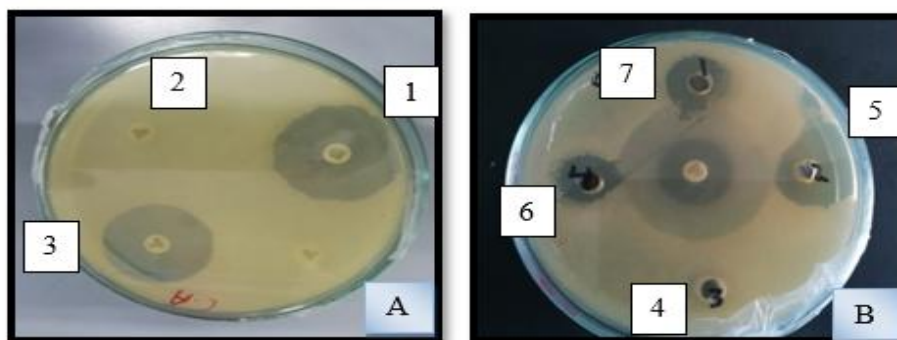


**Figure 12.** A; showing antibiotics zone of inhibition on *C. albicans* and B; showing zone of inhibitions of ST extract, AgNO3 and StAgNPs on *C. albicans*.

**Antilarval Activity**

Antilarval activity of StAgNPs was checked against *Aedes aegypti*, carrier of dengue virus. StAgNPs was Table 4). In 400µg/ml concentration larva was found dead after 5 days but in 1mg/ml concentration larvae become dead after 2 days but other lower

used at different concentrations 50,100,200,400µg/ml and 1mg/ml) (

concentrations do not show any effect on larva even after 1 week as shown in Figure 13.

**Table 4.** Showing antilarval activity of StAgNPs at different concentrations

| Day | (1)<br>Controlled | (2)<br>100µg/ml | (3)<br>200µg/ml | (4)<br>400µg/ml | (5)<br>1mg/ml |
|-----|-------------------|-----------------|-----------------|-----------------|---------------|
| 1   | +                 | +               | +               | +               | +             |
| 2   | +                 | +               | +               | +               | +             |
| 3   | +                 | +               | +               | +               | -             |
| 4   | +                 | +               | +               | +               |               |
| 5   | +                 | +               | +               | +               |               |
| 6   | +                 | +               | +               | -               |               |

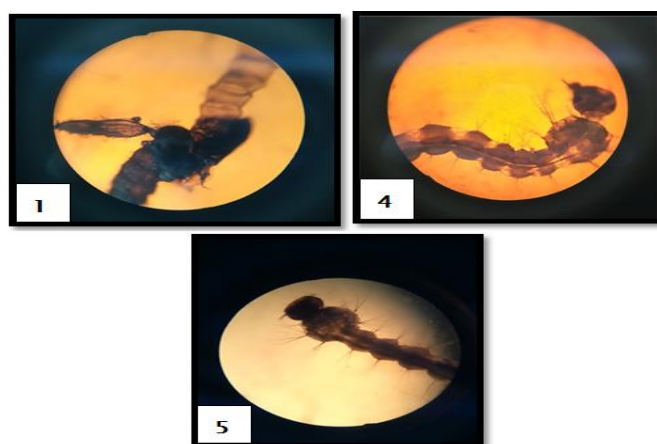


**Figure 13.** (1) Larva develop into adult mosquito, (4) Larva died after 5 days, (5) Larva died after 2 days, (-) showing dead (+) showing alive.

## DISCUSSION

Silver nanoparticles were successfully synthesized from *Solanum tuberosum* peel extract under optimized conditions (10 mM AgNO<sub>3</sub>, 3:7 extract-to-salt ratio, 50 °C, 3 h). In comparison with earlier studies (Tripathi and Sirohi) on synthesis of nanoparticles at lower concentrations and longer incubation periods, the optimized method used in the study ensures nanoparticle formation with maximum yield and good quality, though requiring mild heating. The characteristic color shift from pale yellow to dark brown confirmed AgNP formation, consistent with previous findings reported by Gavarkar *et al.*, 2014. UV–Vis spectra showed a prominent absorption peak at 450 nm, in agreement with studies reporting AgNP peaks between 410–450 nm [(Tahir *et al.*, 2015), (Bhuvanewari *et al.*, 2016) (Al-Ogaidi *et al.*, 2017)] SEM analysis revealed spherical nanoparticles with sizes ranging from 80–100 nm, comparable to earlier studies reporting AgNPs between 50–100 nm (Al-Ogaidi *et al.*, 2017). While smaller particle sizes (20–70 nm) have been reported (Saravanan *et al.*, 2018), (Jacob *et al.*, 2012) the morphology in the present study confirms effective biosynthesis using potato peel extract (Lakshmanan *et al.*, 2017) results from SEM showed that AgNPs having irregular shape having size 5-30nm.

FTIR analysis, peaks at 3245.11 and 1636.16 showed OH from phenolic compounds and Alkenyl bond stretches. Phenolic compounds aromatic acids present in St Extract may be responsible for synthesis and stabilization of StAgNPs (Farvin *et al.*, 2012). Consistent with previous reports (Preetha Devaraj *et al.*, 2013) peaks from 1620 to 1680 showed aromatic alkenyl bending and peaks from 3200 to 3550 showed OH bond stretches from phenolic compounds.

Antimicrobial activity of StAgNPs was checked against gram negative (*E. coli*) and gram positive (*S. aureus*) and *C. albicans*. 100µg and 200µg

concentration was used to check antimicrobial activity. Zone of inhibition shown by 100µg are (16mm, 19mm and 15mm) respectively. The zone of inhibitions shown by 200µg are (20mm, 21mm and 18mm) respectively. The antimicrobial test results by (Tripathi and Sirohi) , used 100µg concentration and zone of inhibitions were in between (7mm to 9.5mm) against *E.coli* and *S.aureus*.

Results from (Dhand, 2016) and (Saravanan, 2018), biosynthesized AgNPs showed significant zone of inhibitions at higher dose against Gram positive and negative bacteria. The antimicrobial activity of biosynthesized AgNPs from plant extract showed zone of inhibitions from 12mm-16mm (Lekshmi *et al.*, 2017). Also, according to (Logeswari *et al.*, 2015) plant induced AgNPs showed 12mm to 25mm zone of inhibition. Antifungal activity of StAgNPs was also determined against *Candida albicans*. StAgNPs showed more activity at 100µg/ml and 200µg/ml as compared to lower concentrations (Mohanta *et al.*, 2017) also showed the antifungal activity of silver nanoparticles synthesized from plant extract.

MIC, MBC & MFC were also checked against *E. coli*, *S. aureus* and *C. albicans*. The minimum amount of StAgNPs to inhibit the growth was 100µg/ml and bactericidal and fungicidal activity was shown by StAgNPs at 200µg. (Amanda Fucci Wady *et al.*, 2014) and (Gnanadesigan *et al.*, 2012) showed higher values of MIC and MBC & MFC against *E. coli*, *S. aureus* and *C. albicans*. The activity of silver nanoparticles is size dependent. Smaller the size greater will be the efficacy of the silver nanoparticles and activity decreases if size increases. Also, according to (Agnihotri *et al.*, 2014) antibacterial activity of silver nanoparticles against bacterial strains increases as the size of AgNPs decreases.

Antilarval activity of StAgNPs was checked against *Aedes aegypti*, carrier of dengue virus. StAgNPs was used at different concentrations

(50,100,200,400 $\mu$ g/ml and 1mg/ml). In 400 $\mu$ g/ml concentration larva was found dead after 5 days but in 1mg/ml concentration larvae become dead after 2 days but other lower concentrations do not show any effect on larva even after 1 week. Similarly (Kumar et al., 2018) reported AgNPs do not have any effect on larva after exposure to AgNPs for 72hrs and (Bhubaneswar et al., 2015) found that the AgNPs at lower concentration do not have any effect on larva. However, more research is needed for the proper anti larval actions of these silver nanoparticles.

#### AUTHOR CONTRIBUTIONS

All authors contributed equally in manuscript writeup and analysis. M.H.M performed all research and wrote the first draft of the article S.R verified all research data and proofread the article.

#### COMPETING OF INTEREST

The authors declare no competing interests.

#### REFERENCES

- Ajitha, B., Reddy, Y.A.K., Jeon, H.-J. and Ahn, C.W. (2018) 'Synthesis of silver nanoparticles in an eco-friendly way using *Phyllanthus amarus* leaf extract: Antimicrobial and catalytic activity', *Advanced Powder Technology*, 29, pp. 86–93.
- Akhtar, M.S., Panwar, J. and Yun, Y.-S. (2013) 'Biogenic synthesis of metallic nanoparticles by plant extracts', *ACS Sustainable Chemistry & Engineering*, 1, pp. 591–602.
- Al-Ogaidi, I., Salman, M.I., Mohammad, F.I., Aguilar, Z., Al-Ogaidi, M., Hadi, Y.A. and Al-Rhman, R.M.A. (2017) 'Antibacterial and cytotoxicity of silver nanoparticles synthesized in green and black tea', *World Journal of Pharmacy and Pharmaceutical Sciences*, 5, pp. 39–45.
- Bhuvanewari, R., Xavier, R.J. and Arumugam, M. (2016) 'Larvicidal property of green synthesized silver nanoparticles against vector mosquitoes (*Anopheles stephensi* and *Aedes aegypti*)', *Journal of King Saud University – Science*, 28, pp. 318–323.
- Das, B., Dash, S.K., Mandal, D., Ghosh, T., Chattopadhyay, S., Tripathy, S., Das, S., Dey, S.K., Das, D. and Roy, S. (2017) 'Green synthesized silver nanoparticles destroy multidrug-resistant bacteria via reactive oxygen species-mediated membrane damage', *Arabian Journal of Chemistry*, 10, pp. 862–876.
- Gavarkar, P., Rahul, S., Shrinivas, K. and Magdum, C. (2014) 'Green synthesis and antimicrobial activity of silver nanoparticles from *Cucumis melo* extract', *International Journal of Universal Pharmacy and Bio Sciences*, 3, pp. 392–396.
- Jacob, S.J.P., Finub, J. and Narayanan, A. (2012) 'Synthesis of silver nanoparticles using *Piper longum* leaf extract and its cytotoxic activity against Hep-2 cell line', *Colloids and Surfaces B: Biointerfaces*, 91, pp. 212–214.
- Kale, R.D. and Jagtap, P. (2018) 'Biogenic synthesis of silver nanoparticles using *Citrus limon* leaves and its structural investigation', in *Advances in Health and Environment Safety*. Singapore: Springer, pp. 211–220.
- Kumar, B., Smita, K., Cumbal, L. and Debut, A. (2017) 'Green synthesis of silver nanoparticles using Andean blackberry fruit extract', *Saudi Journal of Biological Sciences*, 24, pp. 45–50.
- Lakshmanan, G., Sathiyaseelan, A., Kalaichelvan, P. and Murugesan, K. (2017) 'Plant-mediated synthesis of silver nanoparticles using fruit extract of *Cleome viscosa* L.: Assessment of antibacterial and anticancer activity', *Karbala International Journal of Modern Science*, 3, pp. 61–68.
- Ndikau, M., Noah, N.M., Andala, D.M. and Masika, E. (2017) 'Green synthesis and characterization of silver nanoparticles using *Citrullus lanatus* fruit rind extract', *International Journal of Analytical Chemistry*, 2017, Article ID 8108504.
- Pugazhendhi, A., Prabakar, D., Jacob, J.M., Karuppusamy, I. and Saratalé, R.G. (2018) 'Synthesis and characterization of silver nanoparticles using *Gelidium amansii* and their antimicrobial activity against pathogenic bacteria', *Microbial Pathogenesis*, 114, pp. 41–45.
- Saravanan, M., Barik, S.K., MubarakAli, D., Prakash, P. and Pugazhendhi, A. (2018) 'Synthesis of silver nanoparticles from *Bacillus brevis* (NCIM 2533) and their antibacterial activity against pathogenic bacteria', *Microbial Pathogenesis*, 116, pp. 221–228.
- Subbennaik, S.C. (2016) 'Physical and chemical nature of nanoparticles', in *Plant Nanotechnology*. Cham: Springer, pp. 29–45.
- Tahir, K., Nazir, S., Li, B., Khan, A.U., Khan, Z.U.H., Ahmad, A. and Khan, F.U. (2015) 'Efficient photocatalytic activity of green-synthesized silver nanoparticles using *Salvadora persica* stem extract', *Separation and Purification Technology*, 150, pp. 316–324.
- Tripathi, A. and Sirohi, R. (2019) 'Antimicrobial activities of silver nanoparticles synthesized from peels of fruits and vegetables', *Journal of Nanomaterials*, 2019, Article ID 4826375.

